

Quantum frequency conversion with coherent transfer of time-bin encoding

Shushan Petrosyan^{*} and Yuri Malakyan[†]

Institute for Physical Research, Armenian National Academy of Sciences, Ashtarak-2, 0203, Armenia



(Received 23 February 2022; accepted 5 May 2022; published 26 May 2022)

Time-bin encoding of photons offers a robust kind of long-distance quantum communication over lossy channels. The diversity of material nodes in quantum networks operating at natural frequencies requires coherent frequency and wave-form conversion of information-carrying photons to provide an efficient quantum interface with optical fibers and various quantum memories, which has been extensively studied. However, the quantum frequency conversion with transfer of time-bin encoding between single photons of different wavelengths has not yet been explored. In this paper, we present a method for efficiently exchanging time-bin encoding in the conversion process between two photons propagating in cold tripod atoms driven by a strong laser field. The latter is designed to slow down photons and suppress their absorption due to electromagnetically induced transparency. Photons interact parametrically through modified atomic coherence, which is utilized also to achieve equal group velocities of photons. We demonstrate the ability of our model to generate entanglement between distant atoms that equally share the original quantum information stored in the ground-state polarization qubits of both atoms. The proposed method for frequency conversion based on modified atomic coherence is promising because it can simplify the implementation of reliable and high-speed quantum communication protocols based on single-photon entanglement.

DOI: [10.1103/PhysRevA.105.052606](https://doi.org/10.1103/PhysRevA.105.052606)

I. INTRODUCTION

Quantum information encoded in time-bin photonic qubits is preserved over long distances due to the robustness of time-bin superposition against decoherence in optical fibers [1–3], which greatly benefits lossless quantum information sharing among many users at predetermined times with controllable wave forms [4,5]. Besides, the employment of time-bin entangled photons allows linear optical quantum computing (LOQC) to be performed in a single spatial mode [6], providing scalable implementation of multiqubit protocols, without creating unwieldy networks that inevitably arise in all schemes of LOQC [7,8] due to many spatial modes. The time-bin encoding is easily achieved for narrow-band photons at the visible to short near-infrared wavelengths, which are the working wavelengths for the most efficient quantum memories. In order to perform these tasks of quantum information memory processing and transmission over optical fibers, the single photons (SP) of certain wavelengths carrying information from and to memories must be coherently transformed to and from the fiber-optic telecommunication band 1.5 μm , where the photon losses are minimal. In recent decades, a number of experiments have been performed in nonlinear media on quantum frequency conversion (QFC) of broadband photons from the visible and near-infrared ranges to the telecom band [9–17]. Inverse up-conversions are also realized [18–25]. The conversion between the visible and telecom wavelengths has been performed with

narrow-band photons in cold Rb atoms using four-wave mixing (FWM) [26,27]. Furthermore, a number of works have demonstrated the ability of QFCs to retain a broad range of photon properties [9,13,17,18,21,22]. However, QFC that preserves time-bin encoding has not yet been explored. Besides, only few studies have been carried out on the frequency conversion between visible photons (see, for example, Ref. [28]), while the QFC in the visible range is highly demanded for entanglement generation and swapping between nodes of a hybrid quantum network, as the quantum internet [29].

In this paper, we propose and theoretically develop a frequency converter for narrow-band visible photons that aims to solve both problems. In our scheme, the visible photons are efficiently converted into photons of various wavelengths in the visible or telecommunication bands with coherent transfer of time-bin encoding due to three-wave mixing that is triggered by a collective atomic-spin excitation. We consider an ensemble of tripod-type cold atoms (Fig. 1), where the signal and converted photons interact with atoms on the transitions $|1\rangle \rightarrow |3\rangle$ and $|2\rangle \rightarrow |3\rangle$, correspondingly, while a control laser field E_c resonantly driving atoms on the $|4\rangle \rightarrow |3\rangle$ transition slows down the photons and suppresses their absorption due to electromagnetically induced transparency (EIT). The parametric interaction between photons is initiated by a prearranged coherence between two metastable states $|1\rangle$ and $|2\rangle$ (Fig. 1), which acts as an auxiliary field in three-wave mixing with the two quantum fields. For closely spaced levels 1 and 2 separated by several GHz, when the converted photon is also in the visible range, this coherence can be created directly with microwave fields. For the converted photon in the telecom band, the two-photon stimulated Raman transitions can be used for this goal. Although

^{*}shushanpet@gmail.com

[†]yuramalakyan@gmail.com

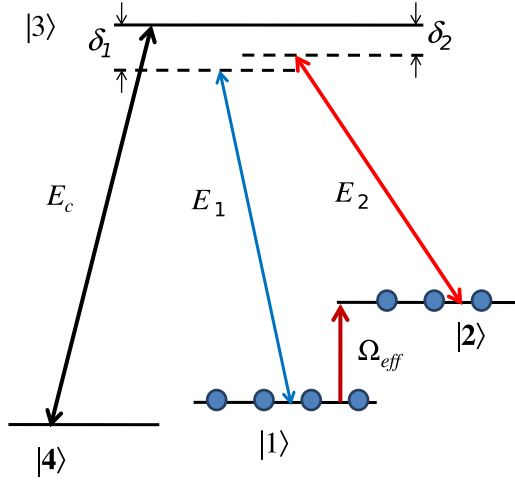


FIG. 1. Tripod level configuration with parametric interaction of two single photons E_1 and E_2 through the coherence between two metastable states $|1\rangle$ and $|2\rangle$ induced by a driving field Ω_{eff} . The Ω_c control field creates electromagnetically induced transparency for photons.

it is difficult to find a tripod-level configuration in neutral atoms with transitions at telecom wavelengths, the solid-state crystals doped with rare-earth ions can provide an important alternative [14,30,31], especially as they are easily integrated into the quantum repeater architecture [32]. It is worth noting an interesting possibility of frequency conversion between infrared photons at wavelengths 1500 and 1100 nm in barium atoms with tripod configuration of four-level manifold ($6s^2$) 1S_0 , ($6s6p$) 1P_1 , ($6s5d$) 1D_2 and ($6s5d$) 3D_2 [33]. Below we carry out a general solution of the problem, which is applicable to all specific situations.

In our model, the prepared coherence is also adjusted appropriately to make the group velocities of the photons equal. In this case, the efficiency of QFC is close to unity, whereas, as shown in Ref. [34], in the general case of unequal group velocities, the frequency conversion ceases after some propagation distance because of the temporal walk-off of photons caused by the group velocity mismatch, which is notably large for slow photons. For the same reason, an imperfect conversion between the visible and telecommunication photons should be expected in the FWM scheme used in Refs. [26,27], if the equality of group velocities of the photons is not ensured. A detailed analysis of this effect is given in Ref. [35]. Note that a tripod medium driven by classical fields and prepared in a coherent superposition of the two ground states of the atoms has been studied with regard to parametric generation of new fields [36]. In this case also, the group velocity mismatch between the driving and newly created fields can significantly reduce the efficiency of the parametric process, especially in the case of short pulses.

In the next section, we present the interaction setup and formulate the theory. We make the necessary approximations providing lossless QFC in our model and analytically solve the propagation equations for quantum field amplitudes. In Sec. III, we examine the coherent transfer of time-bin encoding from the signal to the converted photon for various initial wave forms. Here we also study the storage of time-bin en-

coding in two distant atoms, which provides the transmission of quantum information without loss over long distances. Our conclusions are summarized in Sec. IV.

II. PROPOSED SCHEME

Here we extend the primary tripod system [37] to the case of modified atomic coherence between the two metastable states $|1\rangle$ and $|2\rangle$ (Fig. 1) that engenders the parametric interaction between two quantum fields at the single-photon level, causing a coherent transformation of the frequency and temporal shape of single photons. All the atoms are assumed to be optically pumped, for example, into the state $|1\rangle$, while the state $|4\rangle$ remains always empty. Then, the atoms are prepared in a superposition of the states $|1\rangle$ and $|2\rangle$ by driving the $|1\rangle \rightarrow |2\rangle$ transition either directly with a resonant microwave pulse or by two Raman pulses resonantly exciting the corresponding two-photon transition with an effective pulse area

$$\theta(t) = \int_{-\infty}^t \Omega_{\text{eff}}(t') dt', \quad (1)$$

where $\Omega_{\text{eff}}(t)$ is the Rabi frequency of the microwave field or of the effective field of Raman-coupling laser pulses. Here it is taken into account that the driving pulses are incomparably shorter than the lifetime of metastable states and also, without loss of generality, it is assumed that all Rabi frequencies are real. After turning off the driving fields, the superposition state $|\psi\rangle = \cos \theta(\infty)|1\rangle + \sin \theta(\infty)|2\rangle$ is formed, where the state populations ρ_{ii} , $i = 1, 2$, and induced coherence ρ_{12} are

$$\rho_{11} = \cos^2 \theta(\infty), \quad \rho_{22} = \sin^2 \theta(\infty), \quad (2a)$$

$$\rho_{21} = \rho_{12} = \rho_0 = \sqrt{\rho_{11}\rho_{22}} = \frac{1}{2} \sin 2\theta(\infty). \quad (2b)$$

Since the number of photons in quantum fields is much less than the number of atoms, we can regard the atomic populations ρ_{ii} , $i = 1, 2$, and the coherence ρ_0 as constant throughout the evolution of the system. Obviously, this approximation is valid within the atomic ground-state coherence lifetime.

We describe the quantum fields by slowly varying dimensionless operators $\hat{\mathcal{E}}_i(z, t)$, $i = 1, 2$,

$$\hat{\mathcal{E}}_i(z, t) = \sqrt{\frac{\hbar\omega_i}{2\varepsilon_0 V}} \hat{\mathcal{E}}_i(z, t) \exp[i(k_i z - \omega_i t)] + \text{H.c.},$$

where $V = \pi w_a^2 L$ is the volume of interaction region of the length L and w_a is the width of the atomic transverse distribution. Along with those, the control beam is assumed to have a constant transverse profile, much wider than that of the SP pulses. The operators $\hat{\mathcal{E}}_i(z, t)$, $i = 1, 2$, obey the commutation relations

$$[\hat{\mathcal{E}}_i(z, t), \hat{\mathcal{E}}_j^+(z, t')] = \frac{L}{c} \delta_{ij} \delta(t - t'), \quad (3)$$

which are valid in free space and are preserved in the medium [see below, Eqs. (15)].

The interaction Hamiltonian in the rotating wave picture is given by

$$H = \hbar[\delta_1 \hat{\sigma}_{11} + \delta_2 \hat{\sigma}_{22} - g_1 \hat{\mathcal{E}}_1 \hat{\sigma}_{31} - g_2 \hat{\mathcal{E}}_2 \hat{\sigma}_{32} - \Omega_c \hat{\sigma}_{34} + \text{H.c.}],$$

where $\hat{\sigma}_{ij} = |i\rangle\langle j|$ are the atomic operators, $\delta_i = \omega_i - \omega_{3i}$, $i = 1, 2$, is one-photon detuning and $g_i = \mu_{3i}\sqrt{\frac{\omega_i}{2\hbar\epsilon_0 V}}$ is the atom-photon coupling constant for i th photon, respectively, and $\Omega_c = \mu_{34}E_c/\hbar$ is the Rabi frequency of the control field.

In the slowly varying envelope approximation, the propagation equations for the quantum field operators are given by

$$\left(\frac{\partial}{\partial z} + \frac{1}{c}\frac{\partial}{\partial t}\right)\hat{\mathcal{E}}_i(z, t) = i\frac{g_i}{c}N\hat{\sigma}_{i3}(z, t), \quad (4)$$

where N is the total number of atoms. In the weak field limit $g_i\hat{\mathcal{E}}_i \ll \Omega_c$ and for constant ρ_{ij} , $i, j = 1, 2$ [Eqs. (2)], one can set $\langle\hat{\sigma}_{33}\rangle = \langle\hat{\sigma}_{44}\rangle = \langle\hat{\sigma}_{43}\rangle \simeq 0$. Then the equations for the atomic operators take the form

$$\frac{\partial}{\partial t}\hat{\sigma}_{13} = (i\delta_1 - \Gamma)\hat{\sigma}_{13} + ig_1\hat{\mathcal{E}}_1\rho_{11} + ig_2\hat{\mathcal{E}}_2\rho_{00} + i\Omega_c\hat{\sigma}_{14} + \hat{F}_{13}, \quad (5)$$

$$\frac{\partial}{\partial t}\hat{\sigma}_{14} = (i\delta_1 - \gamma_c)\hat{\sigma}_{14} + i\Omega_c^*\hat{\sigma}_{13} + \hat{F}_{14}. \quad (6)$$

The equations for $\hat{\sigma}_{23}$ and $\hat{\sigma}_{24}$ are similar to Eqs. (5) and (6) with the substitution $1 \leftrightarrow 2$ everywhere. Here 2Γ is the atomic spontaneous decay rate from the upper level 3, γ_c is the ground-state coherence damping rate, and \hat{F}_{ij} are the atomic noise operators associated with relaxations.

Applying the approach developed in Ref. [37], we solve the atomic equations perturbatively with small parameters $g_i\hat{\mathcal{E}}_i/\Omega_c$ and in the adiabatic limit, while preserving the first time derivative of the field amplitudes in order to obtain the correct group velocities of the photons. From Eq. (6), we have

$$\hat{\sigma}_{13} = -\frac{i}{\Omega_c^*}\left(\frac{\partial}{\partial t} - i\delta_1 + \gamma_c\right)\hat{\sigma}_{14} + \frac{i}{\Omega_c^*}\hat{F}_{14}.$$

Substituting this expression into Eq. (5), we solved this equation, neglecting the spin relaxation $\gamma_c \ll \delta_i < \Gamma$ and using the EIT conditions $|\Omega_c|^2 \gg \Gamma\delta_i, \delta_i^2$, $i = 1, 2$. The final solutions for atomic operators are obtained in the following form,

$$\hat{\sigma}_{13} = \frac{g_1\hat{\mathcal{E}}_1\rho_{11}}{|\Omega_c|^2}\left(\delta_1 + i\Gamma\frac{\delta_1^2}{|\Omega_c|^2}\right) + \frac{g_2\hat{\mathcal{E}}_2\rho_{00}\delta_1}{|\Omega_c|^2} + i\frac{g_1\rho_{11}}{|\Omega_c|^2}\frac{\partial\hat{\mathcal{E}}_1}{\partial t} - i\frac{\delta_1}{|\Omega_c|^2}\hat{F}_{13} + i\frac{1}{\Omega_c^*}\hat{F}_{14}, \quad (7a)$$

$$\hat{\sigma}_{14} = -\frac{g_1\hat{\mathcal{E}}_1\rho_{11}}{\Omega_c}\left(1 + i\Gamma\frac{\delta_1}{|\Omega_c|^2}\right) - \frac{g_2\hat{\mathcal{E}}_2\rho_{00}}{\Omega_c} + i\frac{1}{\Omega_c}\hat{F}_{13}, \quad (7b)$$

and

$$\hat{\sigma}_{2(3,4)} = \hat{\sigma}_{1(3,4)}(1 \leftrightarrow 2). \quad (8)$$

For simplicity, we consider the case $\delta_1 = \delta_2 = \delta$. Then the equations for quantum fields are reduced to

$$\left(\frac{\partial}{\partial z} + \frac{1}{v_1}\frac{\partial}{\partial t}\right)\hat{\mathcal{E}}_1 = -\left(\frac{k_1}{2} - i\delta s_1\right)\hat{\mathcal{E}}_1 + i\beta\hat{\mathcal{E}}_2 + \hat{\mathcal{F}}_1, \quad (9)$$

$$\left(\frac{\partial}{\partial z} + \frac{1}{v_2}\frac{\partial}{\partial t}\right)\hat{\mathcal{E}}_2 = -\left(\frac{k_2}{2} - i\delta s_2\right)\hat{\mathcal{E}}_2 + i\beta\hat{\mathcal{E}}_1 + \hat{\mathcal{F}}_2, \quad (10)$$

where

$$k_i = \frac{2g_i^2N\rho_{ii}\Gamma}{c|\Omega_c|^2}\frac{\delta^2}{|\Omega_c|^2}, \quad s_i = \frac{g_i^2N\rho_{ii}}{c|\Omega_c|^2} \quad (11)$$

are, respectively, the linear absorption and phase-modulation coefficients for i th field, $i = 1, 2$,

$$\beta = \frac{g_1g_2N\rho_{00}}{c|\Omega_c|^2}\delta \quad (12)$$

is the constant of parametric interaction between quantum fields gained by the prepared coherence ρ_{00} on the transition $|1\rangle \leftrightarrow |2\rangle$, and

$$v_{1,2} = (1/c + s_{1,2})^{-1} \quad (13)$$

are the group velocities of the photons. The δ -correlated commutator-preserving noise operators $\hat{\mathcal{F}}_{1,2}$ of the fields have the properties [38]

$$\langle\hat{\mathcal{F}}_i(z, t)\rangle = \langle\hat{\mathcal{F}}_i(z, t)\hat{\mathcal{F}}_j(z', t')\rangle = 0, \quad i, j = 1, 2,$$

$$\langle\hat{\mathcal{F}}_i(z, t)\hat{\mathcal{F}}_j^\dagger(z', t')\rangle = 2k_i\delta_{ij}\delta(z - z')\frac{L}{c}\delta(t - t'),$$

indicating that they give no contribution in the absence of photon losses.

The complete conversion of photons is achieved at their equal group velocities $v_1 = v_2 = v$, which occurs if $s_1 = s_2 = s$ or the condition $g_1^2\rho_{11} = g_2^2\rho_{22}$ is satisfied, as can be seen from Eqs. (11) and (13). The implementation of this condition is easily controlled by the pulse area of the driving fields defined in Eq. (1). From the populations of metastable states, we find the required value of $\theta(\infty)$

$$\rho_{11} = \cos^2\theta(\infty) = \frac{g_2^2}{g_1^2 + g_2^2}, \quad \rho_{22} = 1 - \rho_{11}.$$

In this case, the absorption coefficients are also equal $k_1 = k_2 = k$. In what follows, we will require negligible absorption of photons by imposing the condition $kL \ll 1$. In addition, the phase modulation s can be eliminated in Eqs. (9) and (10) upon replacing $\hat{\mathcal{E}}_{1,2} \rightarrow \exp[i\delta s z]\hat{\mathcal{E}}_{1,2}$. Then, the final equations for quantum fields are cast to a simple form

$$\left(\frac{\partial}{\partial z} + \frac{1}{v}\frac{\partial}{\partial t}\right)\hat{\mathcal{E}}_{1,2}(z, t) = i\beta\hat{\mathcal{E}}_{2,1}(z, t), \quad (14)$$

the solution of which in terms of the retarded time $\tau = t - z/v$ depends on the initial amplitudes $\hat{\mathcal{E}}_i(z = 0, \tau) = \hat{\mathcal{E}}_i(\tau)$ as

$$\hat{\mathcal{E}}_i(z, \tau) = \hat{\mathcal{E}}_i(\tau)\cos\beta z + i\hat{\mathcal{E}}_j(\tau)\sin\beta z, \quad i, j = 1, 2, j \neq i, \quad (15)$$

revealing the periodic complete conversion between the photons at the points $z = \frac{\pi}{2\beta}(2n + 1)$, where n is an integer. It is easy to check that $\mathcal{E}_i(z, \tau)$ satisfy the commutation relations in Eq. (3).

The feasibility of our scheme is confirmed by comparing Eqs. (11) and (12), from which it follows that under EIT conditions $k/\beta = 2\Gamma\delta/|\Omega_c|^2 \ll 1$. This allows proper suppression of the absorption of photons, but retainment of their strong parametric interaction.

III. STORAGE OF TIME-BIN ENCODING IN TWO DISTANT ATOMS

A. QFC with coherent transfer of time-bin encoding

Here, we analyze the evolution of an input single-photon state $|\psi_{\text{in}}\rangle = |1_{\omega_1}\rangle|0_{\omega_2}\rangle$, where $|0_{\omega_2}\rangle$ and $|1_{\omega_1}\rangle$ denote

states with zero and one photon, respectively. Similar results are clearly obtained in the case of one input ω_2 -photon and zero photon in the ω_1 field. We assume that initially the ω_1 wave packet is localized around $z = 0$ with a given temporal profile $f_1(t)$,

$$\langle 0 | \hat{\mathcal{E}}_1(0, t) | \psi_{\text{in}} \rangle = \langle 0 | \hat{\mathcal{E}}_1(0, t) | 1_{\omega_1} \rangle | 0_{\omega_2} \rangle = f_1(t),$$

which is normalized as $\frac{c}{L} \int |f_1(t)|^2 dt = 1$, indicating that the number of impinging ω_1 photons is one. Here $|0\rangle = |0_{\omega_1}\rangle |0_{\omega_2}\rangle$ is the vacuum state of the two frequency modes.

In free propagation with velocity v , we have

$$\langle 0 | \hat{\mathcal{E}}_1(0, t - z/v) | 1_1 \rangle = \langle 0 | \hat{\mathcal{E}}_1(\tau) | 1_1 \rangle = f_1(\tau). \quad (16)$$

The dimensionless intensities and mean photon numbers in the single-photon pulses at any distance $0 \leq z \leq L$ are obtained from Eqs. (15) and (16) as

$$I_i(z, \tau) = \langle \psi_{\text{in}} | \hat{\mathcal{E}}_i^\dagger(z, \tau) \hat{\mathcal{E}}_i(z, \tau) | \psi_{\text{in}} \rangle = |\Phi_i(z, \tau)|^2, \quad (17)$$

$$n_i(z) = \langle \psi_{\text{in}} | \hat{n}_i(z) | \psi_{\text{in}} \rangle = \frac{c}{L} \int d\tau I_i(z, \tau) \quad i = 1, 2,$$

where $\Phi_i(z, \tau)$ are the photons' wave functions

$$\begin{aligned} \Phi_1(z, \tau) &= \langle 0 | \hat{\mathcal{E}}_1(z, \tau) | \psi_{\text{in}} \rangle = f_1(\tau) \cos \beta z, \\ \Phi_2(z, \tau) &= \langle 0 | \hat{\mathcal{E}}_2(z, \tau) | \psi_{\text{in}} \rangle = i f_1(\tau) \sin \beta z, \end{aligned} \quad (18)$$

and $\hat{n}_i(z) = \frac{c}{L} \int d\tau \hat{\mathcal{E}}_i^\dagger(z, \tau) \hat{\mathcal{E}}_i(z, \tau)$ are the operators of the number of photons in the modes that pass each point on the z axis in the whole time.

Now, suppose that the input ω_1 photon has a modal structure consisting of temporally separated coherent pulses (time bins), which have, in the general case, different temporal profiles. The latter are localized at time positions $\tau_J > \tau_{J-1} > \dots > \tau_1$ with a separation between them much larger than their lengths such that $f_1(\tau)$ is a coherent superposition of time-bin functions φ_k in the form

$$f_1(\tau) = \sum_{k=1}^J \alpha_k \varphi_k(\tau - \tau_k), \quad (19)$$

where φ_k are real and orthonormal

$$\frac{c}{L} \int \varphi_k(\tau - \tau_k) \varphi_{k'}(\tau - \tau_{k'}) d\tau = \delta_{kk'},$$

and the amplitudes α_k of the probabilities describing the occupation of the corresponding k th temporal mode satisfy

the normalization condition $\sum_{k=1}^J |\alpha_k|^2 = 1$. We believe that the

distance between the temporal bins is significantly greater than the response time of photon detectors, thus providing a direct readout of quantum information encoded in the arrival time of photons. Such states can be created by retrieving a stored photon into multiple time bins, the number of which is evidently limited by the photon coherence time [5,39].

We can describe the input photon with the temporal profile $f_1(t)$ as follows:

$$|1_{\omega_1}; f_1\rangle = \frac{c}{L} \int d\tau f_1(\tau) \hat{\mathcal{E}}_1^\dagger(\tau) |0\rangle. \quad (20)$$

Then, using the unitary mode-transformation Eq. (15), the single-photon state at any point z is obtained in the form

$$|\psi(z)\rangle = \frac{c}{L} \int d\tau f_1(\tau) [\hat{\mathcal{E}}_1^\dagger(\tau) \cos \beta z - i \hat{\mathcal{E}}_2^\dagger(\tau) \sin \beta z] |0\rangle. \quad (21)$$

We assign to each time-bin function φ_k in Eq. (19) a photon creation operator defined by

$$\hat{b}_k^\dagger(\omega_i) = \frac{c}{L} \int d\tau \varphi_k(\tau - \tau_k) \hat{\mathcal{E}}_i^\dagger(\tau), \quad i = 1, 2. \quad (22)$$

These operators obey the commutation relations $[\hat{b}_k(\omega_i), \hat{b}_{k'}^\dagger(\omega_j)] = \delta_{kk'} \delta_{ij}$ and produce one-photon states $\hat{b}_k^\dagger(\omega_{1,2}) |0\rangle = |1_{\omega_{1,2}}; \varphi_k\rangle$.

Substituting Eq. (19) into Eq. (21) and using Eq. (22), we obtain the photon output state in time basis as

$$\begin{aligned} |\psi(L); \text{time}\rangle &= \sum_{k=1}^J \alpha_k [|1_{\omega_1}; \varphi_k\rangle |0_{\omega_2}\rangle \cos \beta L \\ &\quad - i |0_{\omega_1}\rangle |1_{\omega_2}; \varphi_k\rangle \sin \beta L]. \end{aligned} \quad (23)$$

It is seen that the ω_2 photon is generated at $z = L = \pi/(2\beta)$ with a wave form identical to that of the input ω_1 photon, whereas the latter passes into the vacuum state. In the ideal case, the transfer of the time-bin encoding and pulse wave form from the signal photon to the converted one occurs with unit efficiency. In a broader sense, the z dependence of the frequency conversion given by Eq. (23) provides ample opportunities for creating the desired states for both photons. In particular, the QFC is incomplete at $\beta L = \pi/4$, which causes the two frequency modes to share the original time-bin encoding equally, with the desired value of βL being easily regulated by the intensity of the control field, as Eq. (12) implies. As a result, the quantum information encoded in the state of the input photon can be stored in two quantum memories operating at different wavelengths that generates the entangled state of the memory nodes. The fact that a single photon in the superposition of two frequency modes is capable of creating an entangled state, for example, of two separated atoms, thereby revealing the “single-photon” nonlocality, was demonstrated in Ref. [40] in the case of a single-pulse photon. Unlike this simple case, the state (23) contains many separate temporal modes, which are the basis for creating high-dimensional time-bin encoding, thus increasing the resilience of transmitted quantum information to noise.

B. Mapping two-color time-bin qubits into and out of atomic memories

A simple setup demonstrating the ability of the state (23) to distribute the entanglement over long distances is the storage of two time-bin qubits at frequencies ω_1 and ω_2 in two atomic memories with corresponding resonant transitions. The ω_1 photon is stored in a local memory (node A) for further measurement, while the ω_2 photon is directed toward a distant memory (node B) [Fig. 2(a)], where it is subsequently stored, thus creating an entanglement between two memory nodes. The successful entanglement creation needs atomic quantum memories with long storage times. Single-atom-cavity systems with commonly used alkali atoms provide the required

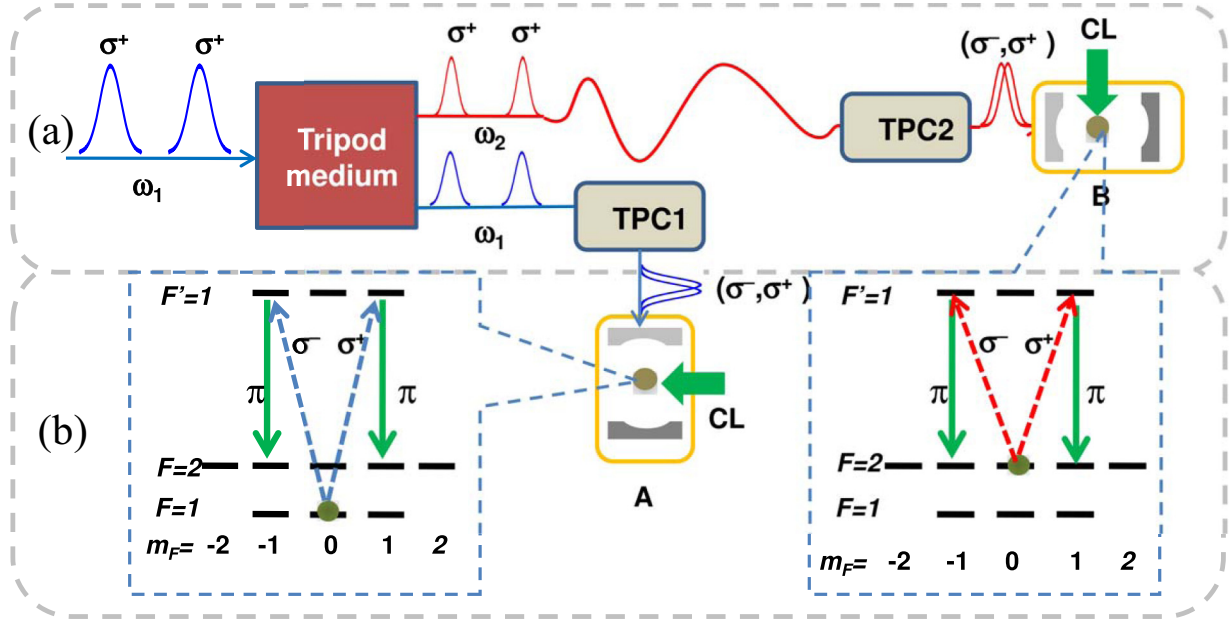


FIG. 2. Experimental procedure for storage of two color time-bin encoding in two distant atoms. (a) At first, the incoming visible ω_1 photon in the state of right-circularly copolarized two time bins is converted in the tripod medium into ω_2 photon with the same time-bin encoding. The two frequency components of the outgoing photon are separated and sent to the local and remote nodes A (ω_1) and B (ω_2), respectively. By passing through the TPC (time-to-polarization converter), the time-bin qubits are converted into the polarization qubits. (b) In each node, the π polarized control laser (CL) converts the superposition of polarization states $|\sigma^+\rangle, |\sigma^-\rangle$ of photons into a superposition of the atomic $F = 2, m_F = \pm 1$ states via a stimulated Raman adiabatic passage

long-lived coherence between the ground hyperfine states, while also featuring the strong atom-photon coupling and high retrieval efficiency [41,42].

The mapping of the state (23) onto the states of single alkali atoms trapped in high-finesse optical cavities at local and remote nodes is carried out in two stages. At first, the time-bin-polarization converter (TPC) transforms the superposition of two temporal modes into the superposition of polarization states for each frequency component of the photon, using only linear optics elements (for similar schemes, see, for example, Refs. [43–45]). Then, the photon polarization qubit is mapped onto the ground-spin state of the corresponding atom via a Raman adiabatic passage using a stimulating laser pulse [Fig. 2(b)].

The microwave field in Fig. 1 is usually chosen to resonantly drive the transition between two clock states $|F = 1, m_F = 0\rangle$ and $|F = 2, m_F = 0\rangle$ of alkali atoms to suppress magnetic-field-induced decoherence. This determines the same polarization of both photons. For definiteness, we consider below the case of right-circularly polarized (σ^+) incoming ω_1 photon. Suppose now that the latter is initially in a superposition of the two temporal modes

$$|1_{\omega_1, \text{in}}\rangle = \alpha_1 |1_{\omega_1}; \varphi_1(\tau - \tau_1)\rangle + \alpha_2 |1_{\omega_1}; \varphi_2(\tau - \tau_2)\rangle,$$

with $\tau_2 > \tau_1$ and $|\alpha_1|^2 + |\alpha_2|^2 = 1$. In the output photon from the tripod medium [Fig. 2(a)], the two frequency components ω_1 and ω_2 are separated and pass through TPC1 and TPC2, respectively. Here, the right-circularly polarized “late” photons (σ^+) are converted to be left-circularly (σ^-) polarized using an electro-optical modulator with a needed modulation period [43]. In addition, the time delay $\tau_2 - \tau_1$ is deleted using an unbalanced Mach-Zender interferometer, thereby

converting the qubit of copolarized time-bin states into the superposition of time-coincident polarization states $|\sigma^+\rangle, |\sigma^-\rangle$ of photons

$$|1_{\omega_i}; \text{polar}\rangle = \alpha_1 |\sigma_{\omega_i}^+\rangle + \alpha_2 |\sigma_{\omega_i}^-\rangle, \quad i = 1, 2. \quad (24)$$

This transforms the final photonic state (23) into a polarization basis of the form

$$|\psi(L); \text{polar}\rangle = |1_{\omega_1}; \text{polar}\rangle |0_{\omega_2}\rangle \cos \beta L - i |0_{\omega_1}\rangle |1_{\omega_2}; \text{polar}\rangle \sin \beta L. \quad (25)$$

At the last step, the generated polarization qubits Eq. (24) are mapped onto a superposition of ground Zeeman states of the atoms, which are prepared in different initial states $|g_A\rangle = |F = 1, m_F = 0\rangle_A$ and $|g_B\rangle = |F = 2, m_F = 0\rangle_B$ [Fig. 2(b)], respectively, while the cavities are correspondingly tuned to the frequencies ω_1 and ω_2 . This is accomplished by applying to each atom a π -polarized control laser pulse resonant to the transition $F' = 1 \rightarrow F = 2$ [41]. The system is initialized in the state $|g_A\rangle \otimes |g_B\rangle \otimes |\psi(L); \text{polar}\rangle$. The control lasers convert the polarization of frequency components Eq. (24) of the photons from $|\psi(L); \text{polar}\rangle$ into the atomic-spin qubits represented by

$$|\psi_{A,B}\rangle = \alpha_1 |F = 2, m_F = 1\rangle_{A,B} + \alpha_2 |F = 2, m_F = -1\rangle_{A,B}. \quad (26)$$

As a result, the entangled state of the two atoms is generated in the form

$$|\Psi_{\text{atom}}\rangle = |\psi_A\rangle \otimes |g_B\rangle \cos \beta L - i |g_A\rangle \otimes |\psi_B\rangle \sin \beta L. \quad (27)$$

The amount of entanglement in the state (27) is controlled by the parameter βL and takes a maximum value at $\beta L = \pi/4$.

Ideally, the discovery of the atom at node A in the $|g_A\rangle$ state heralds the successful encoding of the quantum information carried by the incoming ω_1 photon in the ground-spin state of the remote atom. If the A atom is in the excited state $|\psi_A\rangle$, the remote atom at node B is still ready to receive a photonic qubit at the frequency ω_2 . However, the photon losses in long-distance fiber links limit the rate at which the entanglement generation is successful. Therefore, the entanglement between two remote nodes predicted by Eq. (27) can be verified by simultaneously measuring the states of both atoms, which can be done using known methods for atomic state detection (see, for example, Ref. [46]). This will also allow one to determine the entanglement lifetime. After storage in the atom B, the photon can be retrieved in the polarization state (24) and converted back to a copolarized time-bin qubit with the same initial amplitudes α_1, α_2 by reversing the TPC scheme described above.

IV. CONCLUSIONS

We proposed a fundamentally different mechanism for QFC of narrow-band single photons, which provides a loss-less reversible transfer of high-dimensional time-bin encoding between the photons due to three-wave parametric interaction in the laser-controlled tripod-type atoms. As a result, an incoming single photon ended up in the superposition of two distant frequency modes, each of which is a superposition of

many temporal modes. We demonstrated a novel regime of single-photon entanglement that extends over long distances by storing two time-bin qubits of different wavelengths in two remote atomic memories, which is of key interest for hybrid quantum networks based on the operation of entanglement between photons of different colors. An important advantage of our scheme is to generate in a simple manner any desired entanglement by manipulating the control field intensity and the value of initially prepared atomic coherence. In our approach, unlike many devices used for QFC, the parametric interaction between photons is not based on optical nonlinearities, thus avoiding unwanted background processes usually associated with strong laser fields. In addition, a high-visibility destructive interference of two photons with initially different colors can be observed in our model that provides a different tool for exploiting the Hong-Ou-Mandel interferometry in the frequency domain. Our scheme seems feasible with current technology and could simplify the implementation of quantum communication protocols based on single-photon entanglement.

ACKNOWLEDGMENTS

This work was supported by the RA Science Committee, in the framework of the Research Project No. 20TTAT-QTc004. We also acknowledge financial support from the Basic Foundation of Science of the Government of the Republic of Armenia.

-
- [1] I. Marcikic, H. de Riedmatten, W. Tittel, H. Zbinden, and N. Gisin, *Nature (London)* **421**, 509 (2003).
 - [2] T. Inagaki, N. Matsuda, O. Tadanaga, M. Asobe, and H. Takesue, *Opt. Express* **21**, 23241 (2013).
 - [3] Y. Yu, F. Ma, X.-Y. Luo, B. Jing, P.-F. Sun, R.-Z. Fang, C.-W. Yang, H. Liu, M.-Y. Zheng, X.-P. Xie *et al.*, *Nature (London)* **578**, 240 (2020).
 - [4] M. Hosseini, B. M. Sparkes, G. Hétet, J. J. Longdell, P. K. Lam, and B. C. Buchler, *Nature (London)* **461**, 241 (2009).
 - [5] K. F. Reim, J. Nunn, X.-M. Jin, P. S. Michelberger, T. F. M. Champion, D. G. England, K. C. Lee, W. S. Kolthammer, N. K. Langford, and I. A. Walmsley, *Phys. Rev. Lett.* **108**, 263602 (2012).
 - [6] P. C. Humphreys, B. J. Metcalf, J. B. Spring, M. Moore, X.-M. Jin, M. Barbieri, W. S. Kolthammer, and I. A. Walmsley, *Phys. Rev. Lett.* **111**, 150501 (2013).
 - [7] E. Knill, R. LaFlamme, and G. J. Milburn, *Nature (London)* **409**, 46 (2001).
 - [8] P. Kok, W. J. Munro, K. Nemoto, T. C. Ralph, J. P. Dowling, and G. J. Milburn, *Rev. Mod. Phys.* **79**, 135 (2007).
 - [9] R. Ikuta, Y. Kusaka, T. Kitano, H. Kato, T. Yamamoto, M. Koashi, and N. Imoto, *Nat. Commun.* **2**, 537 (2011).
 - [10] S. Zaske, A. Lenhard, C. A. Keßler, J. Kettler, C. Hepp, C. Arend, R. Albrecht, W.-M. Schulz, M. Jetter, P. Michler, and C. Becher, *Phys. Rev. Lett.* **109**, 147404 (2012).
 - [11] A. S. Clark, S. Shahnia, M. J. Collins, C. Xiong, and B. J. Eggleton, *Opt. Lett.* **38**, 947 (2013).
 - [12] B. Albrecht, P. Farrera, X. Fernandez-Gonzalvo, M. Cristiani, and H. de Riedmatten, *Nat. Commun.* **5**, 3376 (2014).
 - [13] A. Lenhard, J. Brito, M. Bock, C. Becher, and J. Eschner, *Opt. Express* **25**, 11187 (2017).
 - [14] N. Maring, P. Farrera, K. Kutluer, M. Mazzera, G. Heinze, and H. de Riedmatten, *Nature (London)* **551**, 485 (2017).
 - [15] M. Bock, P. Eich, S. Kucera, M. Kreis, A. Lenhard, C. Becher, and J. Eschner, *Nat. Commun.* **9**, 1998 (2018).
 - [16] P. C. Strassmann, A. Martin, N. Gisin, and M. Afzelius, *Opt. Express* **27**, 14298 (2019).
 - [17] C. Morrison *et al.*, *Appl. Phys. Lett.* **118**, 174003 (2021).
 - [18] S. Tanzilli, W. Tittel, M. Halder, O. Alibart, P. Baldi, N. Gisin, and H. Zbinden, *Nature (London)* **437**, 116 (2005).
 - [19] T. Honjo, H. Takesue, H. Kamada, Y. Nishida, O. Tadanaga, M. Asobe, and K. Inoue, *Opt. Express* **15**, 13957 (2007).
 - [20] K. Huang, X. R. Gu, M. Ren, Y. Jian, H. F. Pan, G. Wu, E. Wu, and H. P. Zeng, *Opt. Lett.* **36**, 1722 (2011).
 - [21] S. Ramelow, A. Fedrizzi, A. Poppe, N. K. Langford, and A. Zeilinger, *Phys. Rev. A* **85**, 013845 (2012).
 - [22] W. Liu, N. Wang, Z. Li, and Y. Lia, *Appl. Phys. Lett.* **107**, 231109 (2015).
 - [23] F. Steinlechner, N. Hermosa, V. Pruneri, and J. Torres, *Sci. Rep.* **6**, 21390 (2016).
 - [24] M. Allgaier, V. Ansari, L. Sansoni, C. Eigner, V. Quiring, R. Ricken, G. Harder, B. Brecht, and C. Silberhorn, *Nat. Commun.* **8**, 14288 (2017).
 - [25] H. Rütz, K.-H. Luo, H. Suche, and C. Silberhorn, *Phys. Rev. Applied* **7**, 024021 (2017).
 - [26] A. Radnaev, Y. Dudin, R. Zhao, H. Jen, S. Jenkins, A. Kuzmich, and T. Kennedy, *Nat. Phys.* **6**, 894 (2010).

- [27] Y. O. Dudin, A. G. Radnaev, R. Zhao, J. Z. Blumoff, T. A. B. Kennedy, and A. Kuzmich, *Phys. Rev. Lett.* **105**, 260502 (2010).
- [28] J. D. Sivers, J. Hannegan, and Q. Quraishi, *Phys. Rev. Applied* **11**, 014044 (2019).
- [29] H. J. Kimble, *Nature (London)* **453**, 1023 (2008).
- [30] N. Maring, D. Lago-Rivera, A. Lenhard, G. Heinze, and H. de Riedmatten, *Optica* **5**, 507 (2018).
- [31] K. Zhang, J. He, and J. Wang, *Opt. Express* **28**, 27785 (2020).
- [32] G. Corrielli, A. Seri, M. Mazzera, R. Osellame, and H. de Riedmatten, *Phys. Rev. Applied* **5**, 054013 (2016).
- [33] S. De, U. Dammalapati, K. Jungmann, and L. Willmann, *Phys. Rev. A* **79**, 041402(R) (2009).
- [34] D. Aghamalyan and Y. Malakyan, *Proc. SPIE* **7998**, 799815 (2010).
- [35] A. Gogyan and Y. Malakyan, *Phys. Rev. A* **77**, 033822 (2008).
- [36] E. Paspalakis and P. L. Knight, *J. Mod. Opt.* **49**, 87 (2002); E. Paspalakis, N. J. Kylstra, and P. L. Knight, *Phys. Rev. A* **65**, 053808 (2002).
- [37] D. Petrosyan and Y. P. Malakyan, *Phys. Rev. A* **70**, 023822 (2004).
- [38] M. O. Scully and M. S. Zubairy, *Quantum Optics* (Cambridge University Press, Cambridge, UK, 1997).
- [39] S. Petrosyan and Y. Malakyan, *Phys. Rev. A* **88**, 063817 (2013).
- [40] S. J. van Enk, *Phys. Rev. A* **72**, 064306 (2005).
- [41] S. Ritter, C. Nolleke, C. Hahn, A. Reiserer, A. Neuzner, M. Uphoff, M. Mücke, E. Figueroa, J. Bochmann, and G. Rempe, *Nature (London)* **484**, 195 (2012).
- [42] L. Giannelli, T. Schmit, T. Calarco, C. P. Koch, St. Ritter, and G. Morigi, *New J. Phys.* **20**, 105009 (2018).
- [43] J. S. Hodges, S. P. Pappas, Y. S. Weinstein, and G. Gilbert, in *Conference on Lasers and Electro-Optics (CLEO 2012, San Jose, California, USA)*, OSA Technical Digest (Optica Publishing Group, 2012), paper QF3F.3.
- [44] M. A. M. Versteegh, M. E. Reimer, A. A. van den Berg, G. Juska, V. Dimastrodonato, A. Gocalinska, E. Pelucchi, and V. Zwiller, *Phys. Rev. A* **92**, 033802 (2015).
- [45] C. Kupchak, P. J. Bustard, K. Heshami, J. Erskine, M. Spanner, D. England, and B. Sussman, *Phys. Rev. A* **96**, 053812 (2017).
- [46] J. Volz, R. Gehr, G. Dubois, J. Estève, and J. Reichel, *Nature (London)* **475**, 210 (2011).